Eur. Phys. J. D **42**, 211–216 (2007)
DOI: 10.1140/epjd/e2007-00034-8

THE EUROPEAN
PHYSICAL JOURNAL D

Measurement of the K shell X-ray production cross-sections and fluorescence yields for Nd, Eu, Gd, Dy and Ho using radioisotope X-ray fluorescence in the external magnetic field

D. Demir[a] and Y. Şahin

Department of Physics, Faculty of Arts and Sciences, Ataturk University, 25240 Erzurum, Turkey

Received 18 August 2006 / Received in final form 8 November 2006
Published online 21 February 2007 –

Abstract. The effect of external magnetic field on the K_α and K_β X-ray production cross-sections and K shell fluorescence yields for ferromagnetic elements Nd, Gd and Dy and paramagnetic elements Eu and Ho have been measured at the excitation energy of 59.5 keV γ-rays from ^{241}Am radioactive source of strength 100 mCi in the external magnetic field of intensities ±0.75 T. Furthermore, I_{K_β}/I_{K_α} intensity ratios for these elements have been measured in the external magnetic field. The K X-rays from different targets were detected using a high resolution Si(Li) semiconductor detector. For $B = 0$, the measured K X-ray production cross-sections, K shell fluorescence yields and the I_{K_β}/I_{K_α} intensity ratios were compared with the experimental and theoretical data in literature. The results have shown that the fluorescence parameters as photoionization cross section, fluorescence yield, radiation rates and spectral linewidth can change when the irradiation is conducted in a magnetic field.

PACS. 32.30.Rj X-ray spectra

1 Introduction

Accurate experimental values of X-ray fluorescence (XRF) cross-sections, fluorescence yields and I_{K_β}/I_{K_α} intensity ratios for various elements at various photoionization energies are important because of their extensive use in atomic, molecular, radiation and medical physics, environmental protection and industrial processing. These measurements provide an indirect check on physical parameters, such as K X-ray fluorescence yields, photoionization cross-sections, jump ratios and K X-ray emission rates.

In the recent years, K-shell fluorescence cross-sections and yields have been measured by several investigators using radioisotope and X-ray tubes [1–10]. K X-ray production cross-sections have been determined theoretically for all the elements at energies ranging from 10 to 60 keV [11]. However, limited works in the case of cross-sections of intermediate Z elements have been made at different excitation energies in the interval 8–60 keV [12,13]. K-shell fluorescence yields w_K for different elements have been investigated for many years. Bambynek et al. [14] in a review article have fitted their collection of selected most reliable experimental values in the $13 \leqslant Z \leqslant 92$ range. Krause [15] compiled w_K adopted values for elements $5 \leqslant Z \leqslant 110$. Hubbell et al. [16] have compiled more recent experimental values. Balakrishna et al. [17] measured K fluorescence yields using HPGe low energy photon detector for some rare earth and heavy elements at 59.5 and 279.2 keV γ-rays. The relative K-shell X-ray intensity data are now available in the literature [18].

When the atom is placed in an external magnetic field, the magnetic field produces a torque on the magnetic dipole. The torque is tending to align the dipole with the field, associated with this torque, there is a potential energy of orientation:

$$\Delta E = -\vec{\mu}_l \cdot \vec{B} \tag{1}$$

where μ_l is the orbital magnetic dipole moment of an electron. According to the quantum theory, all spectral lines arise from transitions of electrons between different allowed energy levels within the atom and the frequency of the spectral line is proportional to the energy difference between the initial and final levels. The slight difference in energy is associated with these different orientations in the magnetic field.

In the presence of a magnetic field, the elementary magnetic dipoles, whether permanent or induced, will act to set up a field of induction of their own that will modify the original field. The paramagnetic substances are weakly attracted by the field. Ferromagnetic substances

[a] e-mail: ddemir@atauni.edu.tr

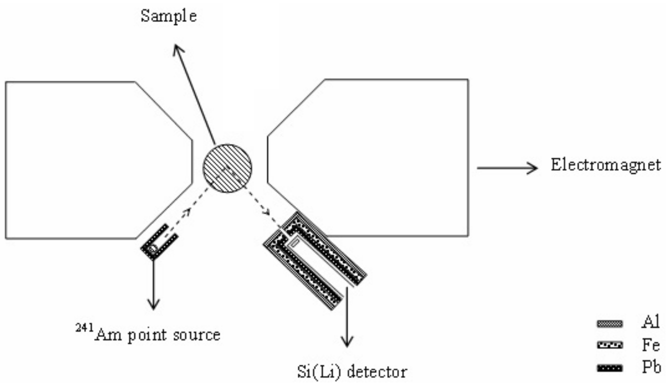

Fig. 1. Experimental setup.

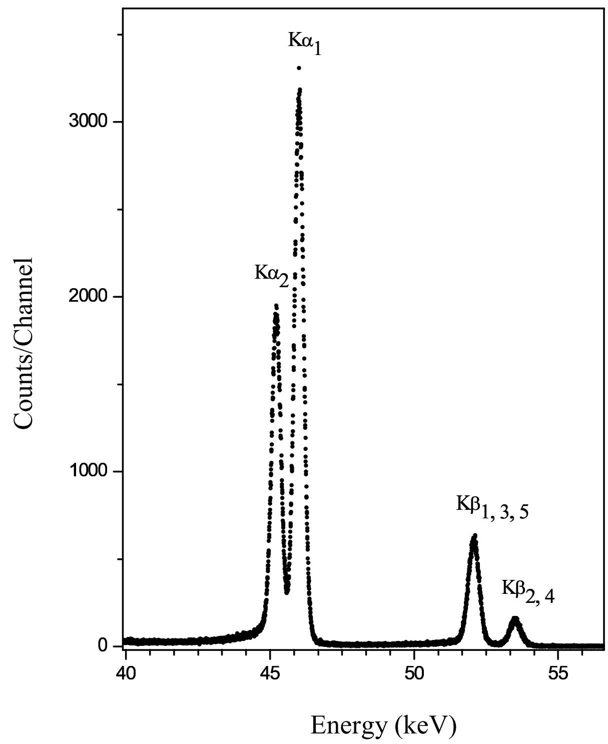

Fig. 2. A typical K X-rays spectrum of the Dy target in +0.75 T magnetic field.

are strongly attracted even by relatively weak fields. Thus, in the presence of the external magnetic field it is expected that both the K shell fluorescence parameters can change and these atomic parameters are different for ferromagnetic and paramagnetic substances due to the magnitude of the magnetic susceptibility is different for both types of substances.

In the present work, to define how the radiative transitions and the structures of the atoms in a strong magnetic field are affected, K_α and K_β X-ray production cross-sections, the K shell fluorescence yields and I_{K_β}/I_{K_α} intensity ratios for ferromagnetic Nd, Gd and Dy and paramagnetic Eu and Ho have been investigated using the 59.5 keV incident photon energy in the external magnetic field of intensities ±0.75 T. The experimental values for $B = 0$ were found to be in agreement with the experimental and theoretical ones. To our knowledge, K shell fluorescence parameters in the external magnetic field have not been reported in the literature and appear to have been measured here for the first time.

2 Experimental details

The geometry and shielding of the experimental set-up are shown in Figure 1. Gamma photons of 59.5 keV from a filtered point source (^{241}Am) of intensity 3.7×10^9 Bq was used for direct excitation of spectroscopically pure foil Gd and Dy and powder Nd, Eu and Ho. The mass thickness of Nd, Gd, Dy, Eu and Ho were 0.2249, 0.0649, 0.0925, 0.2959 and 0.3156 g/cm^2, respectively. The ^{241}Am gamma source was housed at the center of a cylindrical lead shield of 10 mm diameter and 36 mm depth. The samples were placed at a 45° angle with respect to the direct beam and fluorescent X-rays emitted at 90° to the detector. The intensities of gamma rays were measured using a Si(Li) detector having a resolution of 180 eV full width at half maximum at 5.9 keV, an active diameter of 6.2 mm, sensitive crystal depth of 5 mm and a Be window of 0.008 mm thickness. The detector was shielded by a graded filter of Pb, Fe and Al, to obtain a thin beam of photons scattered from the target and to prevent undesirable radiation such as Np L X-rays from ^{241}Am source, L X-rays from the Pb mask, environmental background and background arising from the scattering from the sample holder and electromagnet. The data were collected into 16384 channels of a digital spectrum analyzer DSA-1000. The energy per channel was adjusted as 4 eV to check the peak centroits.

The samples were mounted in a sample holder placed between the pole pieces of an electromagnet capable of producing the magnetic field of ∼3 T at 1 mm pole range. During the study, the magnetic field intensities of ±0.75 T were applied to the samples where + and – represent the relative directions of the magnetic field intensity. The continuity and stability of the currents feeding the electromagnet were checked by an amperemeters. To minimize the systematic and the statistical counting errors arising from radiation emanating from the exciting source, a thin indium wire reference sample was positioned at the collimator of the Si(Li) detector. The accuracy of the detection system was also checked by using the spectra of this reference sample. For each stable value of magnetic field, the pulse height spectrum of K X-rays emitted from each sample was acquired for a period of 10 h to obtain good statistics in the evaluation of each K X-ray peaks and the measurements were repeated 5 times. A typical K X-ray spectrum of Dy at the + 0.75 T is shown in Figure 2. The spectra were analyzed by using Microcal Origin 7.5 Demo Version.

The theoretical values of σ_{K_α} and σ_{K_β} X-ray fluorescence cross-sections were calculated using the equations

$$\sigma_{K_\alpha} = \sigma_K^p(E)\, w_K f_{K_\alpha} \tag{2}$$

$$\sigma_{K_\beta} = \sigma_K^p(E)\, w_K f_{K_\beta} \tag{3}$$

where $\sigma_K^p(E)$ is the K shell photoionization cross-section for the given element at the excitation energy E, w_K is the K shell fluorescence yield and f_{K_a} and f_{K_β} are fractional X-ray emission rates for K_α and K_β X-rays and are defined as

$$f_{K_a} = \left[1 + I_{K_\beta}/I_{K_\alpha}\right]^{-1} \tag{4}$$

$$f_{K_\beta} = \left[1 + I_{K_\beta}/I_{K_\alpha}\right]^{-1} \tag{5}$$

where I_{K_β}/I_{K_α} is the K_β to K_α X-ray intensity ratio. In the present calculations, the values of $\sigma_K^p(E)$ were taken from Scofield [19] based on Hartree-Slater potential theory and the values of w_K were taken from the tables of Hubbell et al. [16]. I_{K_β}/I_{K_α} values based on relativistic Hartree-Slater theory were used for the evaluation of theoretical K X-ray fluorescence cross-sections [20]. The experimental K X-ray fluorescence (XRF) cross-sections $\sigma_{K_i}^x$ were evaluated using the relation

$$\sigma_{K_i}^x = \frac{N_{K_i}}{I_0 G \varepsilon_{K_i} m \beta} \tag{6}$$

where N_{K_i} $(i = \alpha, \beta)$ is the net number of counts under the corresponding photopeak, the product $I_0 G$ is the intensity of the exciting radiation falling on the area of the target samples visible to the detector, ε_{K_i} is the detector efficiency for K_i X-rays, m is the areal mass of the sample in g/cm^2 and β is the self-absorption correction factor for the incident photons and emitted K X-ray photons. β was calculated using the relation

$$\beta = \frac{1 - \exp[-(\mu_{inc}/\cos\theta_1 + \mu_{emt}/\cos\theta_2)m]}{(\mu_{inc}/\cos\theta_1 + \mu_{emt}/\cos\theta_2)m} \tag{7}$$

where μ_{inc} and μ_{emt} are the attenuation coefficients (cm^2/g) of incident photons and emitted characteristic X-rays, respectively (from XCOM [21]). The angles of incident photons and emitted X-rays with respect to the normal at the surface of the sample θ_1 and θ_2 were equal to 45° in the present setup.

The values of the factors $I_0 G \varepsilon_{K_i}$, which contain terms related to the incident photon flux, geometrical factor and the efficiency of the X-ray detector, were determined by collecting the K X-ray spectra of thin samples of Ag, In, Cs, Gd, Ho and W with the mass thickness 0.060–0.38 g/cm^2 in the same geometry in which the K X-ray fluorescence cross-sections were measured and using the equation

$$I_0 G \varepsilon_{K_\alpha} = \frac{N_{K_\alpha}}{\sigma_{K_\alpha} m \beta_{K_\alpha}} \tag{8}$$

where N_{K_a} is the net number of counts under the corresponding photopeak, ε_{K_a} is the detector efficiency for K_α X-rays and β_{K_α} is the self-absorption correction factor

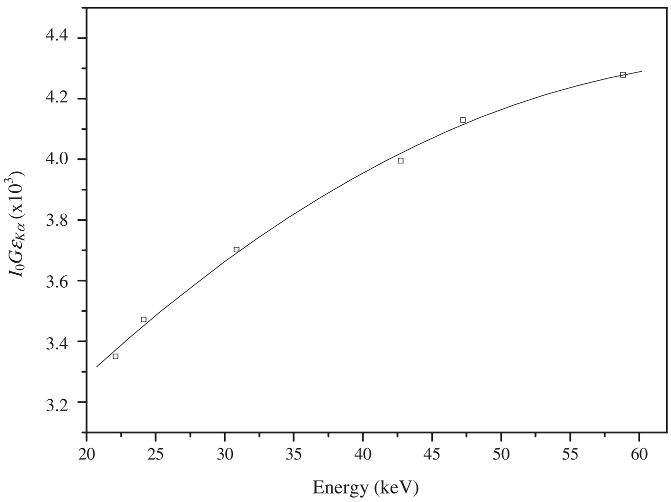

Fig. 3. The factor $I_0 G \varepsilon_{K_\alpha}$ as a function of a mean K X-ray energy.

for the incident photons and emitted K_α X-ray photons. The measured $I_0 G \varepsilon_{K\alpha}$ values for the present geometry are plotted as a function of the mean K X-ray energy as shown in Figure 3.

The experimental K shell X-ray intensity ratios I_{K_β}/I_{K_α} were evaluated using the equation

$$\frac{I_{K_\beta}}{I_{K_\alpha}} = \frac{N_{K_\beta}}{N_{K_\alpha}} \frac{\beta_{K_\alpha}}{\beta_{K_\beta}} \frac{\varepsilon_{K_\alpha}}{\varepsilon_{K_\beta}} \tag{9}$$

where N_{K_α} and N_{K_β} represent the counts under the K_α and K_β peaks, respectively, $\beta_{K_a}/\beta_{K_\beta}$ is the ratio of the self-absorption correction factors of the target and $\varepsilon_{K_a}/\varepsilon_{K_\beta}$ is the ratio of the detector-efficiency values for the K_α and K_β X-rays, respectively.

The fluorescence yield of an atomic shell or subshell is defined as the probability that a vacancy in that shell or subshell is filled through a radiative transition. Thus, for a sample containing many atoms, the fluorescence yield of a shell is equal to the number of photons emitted when vacancies in the shell are filled divided by the number of primary vacancies in the shell. The K-shell fluorescence yields were measured using the relation:

$$w_K = \frac{\sigma_K^x}{\sigma_K^p(E)} \tag{10}$$

where σ_K^x is the total K shell X-ray production cross-section and $\sigma_K^p(E)$ is the K shell photoionization cross-section taken from the tables published by Scofield [19]. The K shell level widths were determined using following equation

$$\Gamma_K = \frac{\Gamma_K(R)}{\omega_K} \tag{11}$$

where $\Gamma_K(R)$ is the radiative transition rates of K shell [22].

Table 1. Experimental, theoretical and fitted K_α X-ray fluorescence cross-sections (b/atom).

Z	element	σ_{K_α} (E) $B = 0$	$B = +0.75$ T	$B = -0.75$ T	σ_{K_α} (T)	fitted (for $B = 0$)
60	Nd	1547 ± 81	1587 ± 92	1587 ± 92	1504	1540
63	Eu	1809 ± 92	1828 ± 98	1827 ± 97	1774	1760
64	Gd	1880 ± 110	1930 ± 121	1931 ± 98	1869	1850
66	Dy	2015 ± 113	2069 ± 132	2068 ± 133	2063	2068
67	Ho	2250 ± 120	2263 ± 131	2262 ± 132	2218	2187

(E) means experimentally; (T) means theoretically.

Table 2. Experimental, theoretical and fitted K_β X-ray fluorescence cross-sections (b/atom).

Z	element	σ_{K_β} (E) $B = 0$	$B = +0.75$ T	$B = -0.75$ T	σ_{K_α} (T)	fitted (for $B = 0$)
60	Nd	374 ± 30	396 ± 38	396 ± 38	354	346
63	Eu	432 ± 32	439 ± 34	439 ± 34	427	434
64	Gd	465 ± 41	480 ± 49	479 ± 48	453	469
66	Dy	559 ± 34	575 ± 41	575 ± 41	505	547
67	Ho	584 ± 43	592 ± 48	591 ± 47	546	591

(E) means experimentally; (T) means theoretically.

3 Result and discussion

In order to reduce the statistical error, five spectra were recorded for each target and magnetic field intensity. The standard deviation of five repeated measurements obtained with the application of $B = +0.75$ T for Nd is 0.98% of the arithmetic mean of these measurements. For $B = -0.75$, this ratio is 1.64. This means that the fluctuation of each measured value about the mean of each series or the statistical counting errors is small.

The overall error in the measured K XRF cross-sections is estimated to be less than 12%. This error is the sum of the uncertainties in different parameters used to calculate the K X-ray production cross-sections, namely, the evaluation of peak areas ($\leqslant$2%), $I_0 G \varepsilon_{K_\alpha}$ product (5–7%), target thickness measurements ($\leqslant$5%), the increasing of the temperature of the electromagnet ($\leqslant$1%) and in the absorption correction factor ($\leqslant$2%).

The experimental values of K_α and K_β X-ray production cross-sections for five elements at 59.54 keV are listed in Tables 1 and 2 together with the theoretical values. Our experimental values for $B = 0$ were fitted to a second order polynomial as a function of atomic number $Z\,(\sum A_n Z^n)$ and fitted values of K XRF cross-sections listed in the same tables. Using these fitted values, the required experimental K shell cross-sections for individual elements can be obtained for comparison and the fit will be valid in the atomic range $60 \leqslant Z \leqslant 67$. It can be seen from Tables 1 and 2 that our measurement values for $B = 0$ are in good agreement, within the experimental uncertainties, with the calculated theoretical values. In the absence of a magnetic field, the agreement between the experimental results and theoretical predictions are within the range 0.5–2.9% for K_α X-ray production cross-sections and 1.2–10.0% for K_β X-ray production cross-sections.

To the best of our knowledge, no other experimental data are available for comparison with the results obtained by us for $B \neq 0$. The measured values of K shell X-ray production cross-sections for the same magnitude but opposite direction of the magnetic field is almost symmetrical as seen from Tables 1 and 2. This is an expected result; since there will be a tendency for the magnetic dipole moment of an atom to align about the direction of the applied magnetic field, such that the orientational potential energy is minimum. Since the effects of the magnetic field are small relative to the uncertainty on the measurements, we applied the t-test to the measured values of K_α X-ray production cross-sections for $B = 0$ and $B = +0.75$ T. It was found that t_{expt} is 3.165 for Nd. The critical t value is 1.860 at the 5% level of significance and 8 degrees of freedom. According to the t-test result, the difference of the means of σ_{K_α} obtained for $B = 0$ and $B = +0.75$ T is significantly different than the t-test difference. We can say that the data collected in Table 1 (and used for producing other tables) shows sensitivity with respect to the magnetic field. As seen from Tables 1 and 2 K_α and K_β X-ray production cross-sections increase in the external magnetic field. Furthermore, the change with the external magnetic field of K X-ray production cross-sections for ferromagnetic Nd, Gd and Dy are greater than that of paramagnetic Eu and Ho.

The measured values of the K shell fluorescence yield w_K in elements Nd, Eu, Gd, Dy and Ho are compared with the calculated values [23] and semiempirical fits [14–16] in Tables 3 and 4. The theoretical values reported by Chen et al. are available for three of the elements studied in the present work. For $B = 0$, the agreement between the present results and theoretical predictions of Chen et al. is within the range 1.4–2.6%. The comparison between the experimental results and the theoretical values leads to the conclusion that either the experimental or the calculated

Table 3. Present experimental results and theoretical predictions of w_K.

Z	element	$B = 0$	$B = +0.75$ T	$B = -0.75$ T	Theory [23]
60	Nd	0.9420 ± 0.057	0.9665 ± 0.045	0.9665 ± 0.045	0.918
63	Eu	0.9435 ± 0.045	0.9535 ± 0.052	0.9531 ± 0.053	0.929
64	Gd	0.9452 ± 0.042	0.9703 ± 0.092	0.9708 ± 0.093	-
66	Dy	0.9564 ± 0.039	0.9820 ± 0.058	$0.9815 \pm .0.062$	-
67	Ho	0.9534 ± 0.057	0.9589 ± 0.069	0.9585 ± 0.071	0.940

Table 4. Present experimental results and semiempirical fits values of w_K.

				Semiempirical values		
Z	element	present work	fitted values	Bambynek (1972)	Krause (1979)	Hubbell (1994)
60	Nd	0.9420 ± 0.057	0.9418	0.920	0.921	0.947
63	Eu	0.9435 ± 0.045	0.9445	0.931	0.932	0.962
64	Gd	0.9452 ± 0.042	0.9467	0.934	0.935	0.966
66	Dy	0.9564 ± 0.039	0.9525	0.940	0.941	0.972
67	Ho	0.9534 ± 0.057	0.9562	0.943	0.944	0.975

Table 5. K shell X-ray intensity ratios I_{K_β}/I_{K_α}.

Z	element	$B = 0$	$B = +0.75$ T	$B = -0.75$ T	theory [22]
60	Nd	0.2418 ± 0.006	0.2495 ± 0.015	0.2495 ± 0.015	0.2355
63	Eu	0.2388 ± 0.015	0.2402 ± 0.003	0.2403 ± 0.003	0.2405
64	Gd	0.2473 ± 0.005	0.2487 ± 0.006	0.2481 ± 0.006	0.2427
66	Dy	0.2774 ± 0.030	0.2779 ± 0.003	$0.2780 \pm .0.003$	0.2449
67	Ho	0.2596 ± 0.013	0.2616 ± 0.004	0.2613 ± 0.004	0.2463

Table 6. The experimental level widths of K shell in the external magnetic field.

Z	element	$B = 0$	$B = +0.75$ T	$B = -0.75$ T	theory [23]
60	Nd	16.48 ± 0.9	16.08 ± 0.8	16.08 ± 0.8	17.36
63	Eu	20.21 ± 0.8	20.00 ± 0.7	20.01 ± 0.7	21.05
64	Gd	21.57 ± 0.8	21.01 ± 0.7	21.00 ± 0.7	-
66	Dy	24.25 ± 0.6	23.62 ± 0.5	23.63 ± 0.5	-
67	Ho	25.91 ± 1.1	25.76 ± 1.0	25.77 ± 1.0	26.87

cross-sections can be used with confidence for analytical purposes and satisfactory for many other applications employing the fundamental parameter approach. Our experimental data for $B = 0$ were fitted to a second order polynomial as a function of atomic number and fitted values of K shell fluorescence yield w_K for all elements listed in the Table 4. The experimental results agree within 0.02–0.2% with the K fluorescence yields calculated using a semiempirical expression. It is clear from Table 3 that the investigated K shell fluorescence yields are symmetrical as expected for the same magnitude but opposite direction of the magnetic field and K shell fluorescence yield increase in the external magnetic field. Furthermore, the change with the external magnetic field of K shell fluorescence yield for ferromagnetic Nd, Gd and Dy are greater than that of paramagnetic Eu and Ho.

For $B = 0$, the present measured K shell X-ray intensity ratios I_{K_β}/I_{K_α} are compared in Table 5 with the theoretical prediction [22]. The agreement between the present results and theoretical prediction of Scofield is within the range 0.7–11.7%. As seen from Table 5 the investigated K shell X-ray intensity ratios I_{K_β}/I_{K_α} are symmetrical as expected for the same magnitude but opposite direction of the magnetic field. Furthermore, the variation with the external magnetic field of K shells X-ray intensity ratios I_{K_β}/I_{K_α} for ferromagnetic elements studied in the present work are greater than that of the studied paramagnetic elements.

The experimental values of K shell level widths are listed in Table 6. The theoretical values reported by Chen et al. are available for three of the elements studied in the present work. For $B = 0$, the agreement between the present results and theoretical prediction [23] are within the range 3.5–5.0%. It can be seen from Table 6 that the experimental values of K shell level widths are symmetrical as expected for $B = +0.75$ and $B = -0.75$ and K shell level widths decrease in the external magnetic field. The results show that the transition probabilities K shell change in the external magnetic field, as well.

As the result, we can say that two important results have been obtained in this work: (i) the K shell fluorescence parameters change when the irradiated atom is in the external magnetic field. This result arise since the final and initial states of the atom relevant to the X-ray transition may have an aligned vacancy if the angular momenta of the states are larger than 1/2. Thus, when an atom is excited by an unpolarized photon beam in the presence of an external magnetic field, joint action of hyperfine interaction and the external magnetic field directed along the unpolarized exciting photon beam caused appearance of an orientation along the magnetic field direction. (ii) The change with the external magnetic field of the K shell fluorescence parameters are different for both types of magnetic substances as K shell fluorescence yield for ferromagnetic Nd, Gd and Dy are greater than that of paramagnetic Eu and Ho. This result arise from the ferromagnetic materials have a large susceptibility ($\simeq 10^5$) to the external magnetic field, while paramagnetic materials have a weak susceptibility ($\simeq 10^{-4}$) to magnetic field.

References

1. D.V. Rao, R. Cesareo, G.E. Gigante, X-ray Spectrom. **22**, 401 (1993)
2. I.A. Al-Nasr, I.J. Jabr, K.A. Al-Saleh, N.S. Saleh, Appl. Phys. A **43**, 71 (1987)
3. R. Durak, Y. Ozdemir, Radiat. Phys. Chem. **61**, 19 (2001)
4. G. Apaydın, E. Tıraşoglu, Nucl. Instr. Meth. B **246**, 303 (2006)
5. S. Seven, Turk J. Phys. **26**, 483 (2002)
6. A.S. Bennal, P.D. Shidling, N.M. Badiger, S.R. Thontadarya, B. Hanumaiah, Am. J. Phys. **73**, 883 (2005)
7. S.B. Gudennavar, N.M. Badiger, S.R. Thontadarya, B. Hanumaiah, Radiat. Phys. Chem. **68**, 721 (2003)
8. T. Yashoda, S. Krishnaveni, R. Gowda, Nucl. Instr. Meth. B **240**, 607 (2005)
9. M.M Be, M.C. Lepy, J. Plagnard, B. Duchemin, Appl. Rad. Isotopes **49**, 1367 (1998)
10. M. Hajivaliei, S. Puri, M.L. Garg, D. Mehta, A. Kumar, S.K. Chamoli, D.K. Avasthi, A. Mandal, T.K. Nandi, K.P. Singh, N. Singh, I.M. Govil, Nucl. Instr. Meth. B **160**, 203 (2000)
11. M.O. Krause, C.V. Nester, C.J. Sparks, E. Ricci, *X-ray fluorescence cross-sections for K and L X-Rays of elements*, Oak Ridge National Laboratory, Report ORNL-5399 (1978)
12. S. Singh, R. Rani, D. Mehta, N. Singh, P.C. Mangal, P.N. Trehan, X-ray Spectrom. **19**, 155 (1990)
13. E. Casnati, C. Baraldi, A. Tartari, Phys. Rev. A **44**, 1699 (1991)
14. W. Bambynek, B. Crasemann, R.W. Fink, H.U. Freund, H. Mark, C.D. Swift, R.E. Price, P.V. Rao, Rev. Mod. Phys. **44**, 716 (1972)
15. M.O. Krause, J. Phys. Chem. Ref. Data **8**, 307 (1979)
16. J.H. Hubbell, P.N. Trehan, N. Singh, B. Chand, D. Mehta, M.L. Garg, R.R. Garg, S. Singh, S. Puri, J. Phys. Chem. Ref. Data **23**, 339 (1994)
17. K.M. Balakrishna, N.G. Nayak, L. Ligappa, K. Siddappa, J. Phys. B **27**, 715 (1994)
18. O. Dogan, O. Simsek, U. Turgut, M. Ertugrul, J. Rad. Nucl. Chem. **232**, 143 (1998)
19. J.H. Scofield, *Theoretical photoionization cross-sections from 1 to 1500 keV*, Lawrence Livermore Laboratory, Report No. UCRL-51326 (1973)
20. J.H. Scofield, At. Nucl. Data Tables **14**, 121 (1974)
21. L. Gerward, N. Guilbert, K. Bjorn, H. Levring, Radiat. Phys. Chem. **60**, 23 (2001)
22. J.H. Scofield, *Theoretical radiative transition rates for K and L shell X-Rays*, Lawrence Livermore Laboratory, Report No. UCRL-51231 (1972)
23. M.H. Chen, B. Crasemann, H. Mark, Phys. Rev. A **21**, 436 (1980)